

# UC Santa Cruz

## UC Santa Cruz Previously Published Works

### Title

The synergetic interaction between LiNO<sub>3</sub> and lithium polysulfides for suppressing shuttle effect of lithium-sulfur batteries

### Permalink

<https://escholarship.org/uc/item/0g74r6tq>

### Authors

Zhang, Liang  
Ling, Min  
Feng, Jun  
[et al.](#)

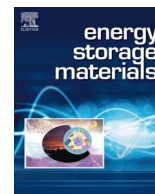
### Publication Date

2018-03-01

### DOI

10.1016/j.ensm.2017.09.001

Peer reviewed



# The synergetic interaction between $\text{LiNO}_3$ and lithium polysulfides for suppressing shuttle effect of lithium-sulfur batteries



Liang Zhang<sup>a,1</sup>, Min Ling<sup>b,1</sup>, Jun Feng<sup>a</sup>, Liqiang Mai<sup>c</sup>, Gao Liu<sup>b,\*</sup>, Jinghua Guo<sup>a,d,\*\*</sup>

<sup>a</sup> Advanced Light Source, Lawrence Berkeley National Laboratory, Berkeley, CA 94720, USA

<sup>b</sup> Applied Energy Material Groups, Energy Storage and Distributed Division, Lawrence Berkeley National Laboratory, Berkeley, CA 94720, USA

<sup>c</sup> State Key Laboratory of Advanced Technology for Materials Synthesis and Processing, Wuhan University of Technology, Wuhan 430070, China

<sup>d</sup> Department of Chemistry and Biochemistry, University of California, Santa Cruz, CA 95064, USA

## ARTICLE INFO

### Keywords:

Lithium anode  
Energy storage  
Sulfur  
In-situ and operando  
X-ray absorption spectroscopy

## ABSTRACT

$\text{LiNO}_3$  has been widely used as an effective electrolyte additive in lithium-sulfur (Li-S) batteries to suppress the polysulfide shuttle effect. To better understand the mechanism of suppressed shuttle effect by  $\text{LiNO}_3$ , herein we report a comprehensive investigation of the influence of  $\text{LiNO}_3$  additive on the formation process of the solid electrolyte interphase (SEI) layer on lithium anode of Li-S batteries by *operando* X-ray absorption spectroscopy (XAS). We observed that a compact and stable SEI layer composed of  $\text{Li}_2\text{SO}_3$  and  $\text{Li}_2\text{SO}_4$  on top of lithium anode is formed during the initial discharge process due to the synergetic effect of shuttled polysulfides and  $\text{LiNO}_3$ , which can effectively suppress the subsequent reaction between polysulfides in electrolyte and lithium metal and thus result in the alleviation of polysulfide shuttle effect. In contrast, when using electrolyte without  $\text{LiNO}_3$ , the shuttled polysulfides continuously react with lithium metal to form insulating  $\text{Li}_2\text{S}$  on lithium anode, leading to the irreversible capacity loss. Our present *operando* XAS study provides a valuable insight into the important role of  $\text{LiNO}_3$  for the protection of lithium anodes, which will be beneficial for the further development of new electrolyte additives for high-performance Li-S batteries.

## 1. Introduction

Lithium-sulfur (Li-S) batteries have attracted extensive attention for energy storage because they can yield rather high specific capacity of 1675 mA h/g ( $16\text{Li} + \text{S}_8 \rightarrow 8\text{Li}_2\text{S}$ ) and specific energy of 2600 W h/kg, indicating a superior energy storage capability [1–9]. In addition, sulfur has the features of light weight, high natural abundance, low cost and environmental benignity. Despite these advantages, the practical application of Li-S batteries is hindered by the rapid capacity degradation upon cycling and low Coulombic efficiency, mainly due to the notorious polysulfide shuttle effect [1,2]. The shuttle effect mainly arises from side reaction between the intermediate polysulfides formed throughout discharge/charge processes and the lithium anode.

$\text{LiNO}_3$  has been widely used as an effective electrolyte additive in Li-S batteries to suppress the polysulfide shuttle effect and thus to improve the cycling performance of Li-S batteries [10–19]. However, the mechanism of this improvement has not been fully understood yet. It is generally believed that  $\text{LiNO}_3$  participates in the formation of solid electrolyte interphase (SEI) film on the surface of lithium anode: it can

not only react with lithium to form a robust surface layer of insoluble  $\text{Li}_x\text{NO}_y$  but also oxidize polysulfides to form  $\text{Li}_x\text{SO}_y$ . Both surface species effectively passivate the lithium anode and therefore the internal redox reaction between soluble polysulfides and lithium anode is impeded [11,12,20–22]. However, Xu et al. claimed that the inhibition of shuttle effect by the  $\text{LiNO}_3$  additive is due to the continuous reaction of  $\text{LiNO}_3$  with lithium anode and/or reduced polysulfides rather than the formation of a stable passivation layer on lithium anode [23].

The reaction product of  $\text{LiNO}_3$  as well as its influence on the formation of SEI layer on lithium anode has been extensively investigated by *ex situ* microscopy (e.g., scanning electron microscope (SEM) and atomic force microscope (AFM)) and *ex situ* spectroscopy (e.g., X-ray photoemission spectroscopy (XPS) and Fourier transformed infrared spectroscopy (FTIR)) [13,20,21,24]. However, due to the highly reactive nature of lithium anode, *ex situ* analysis results may not always be reliable [25]. For instance, the lithium anode could react with the surrounding environment when it is removed from electrolyte solutions and washed by solvents. Therefore, *in situ* and *operando* experiments

\* Corresponding author at: Applied Energy Material Groups, Energy Storage and Distributed Division, Lawrence Berkeley National Laboratory, Berkeley, CA 94720, USA

\*\* Corresponding author at: Advanced Light Source, Lawrence Berkeley National Laboratory, Berkeley, CA 94720, USA

E-mail addresses: [gliu@lbl.gov](mailto:gliu@lbl.gov) (G. Liu), [jguo@lbl.gov](mailto:jguo@lbl.gov) (J. Guo).

<sup>1</sup> These two authors contributed equally to this work.

are highly desired to gain a better mechanistic understanding of the role of  $\text{LiNO}_3$  in the surface chemistry of lithium anode [26]. Although a few *in situ* and *operando* SEM and optical microscopy studies to investigate the passivation of lithium metal using  $\text{Li}_2\text{S}_8$  and  $\text{LiNO}_3$  as co-additives in the electrolyte have been reported [13,27], the formation process of the SEI layer on lithium anode in a working Li-S battery with and without  $\text{LiNO}_3$  additive has seldom been studied [28]. In this work, we have systematically investigated the formation process of the SEI layer on lithium anode with and without  $\text{LiNO}_3$  additive in electrolyte for Li-S cells by *operando* S K-edge X-ray absorption spectroscopy (XAS) throughout the first discharge process. The advantage of XAS is that it is element-resolved and sensitive to the local chemical bonding environment and solvent environment [29]. *Operando* XAS method has been widely used to investigate the reaction mechanism of sulfur cathode during the charge/discharge processes previously [24,30–35]. For example, we have investigated the electrochemical charging mechanism of  $\text{Li}_2\text{S}$  by using *operando* S K-edge XAS in our previous report [35]. In contrast, the present study explores the sulfur speciation in electrolyte and lithium anode by using a specially designed coin cell (Figure S1 in Supporting information) to characterize the role of  $\text{LiNO}_3$  in the formation process of the SEI layer on lithium anodes. By using electrochemistry investigation, morphology characterization and *operando* XAS, we have found that  $\text{LiNO}_3$  and intermediate polysulfides formed during the discharge process enable a synergetic effect and lead to the formation of a stable SEI layer with  $\text{Li}_2\text{SO}_3$  and  $\text{Li}_2\text{SO}_4$  on top, which can effectively alleviate the shuttle effect and thus improve the cycling performance of Li-S cells.

## 2. Results and discussion

Fig. 1a shows the galvanostatic cycling performances of Li-S cells with and without 2 wt%  $\text{LiNO}_3$  additive in the electrolyte. An initial discharge capacity of 1026.7 mA h/g is achieved when using  $\text{LiNO}_3$  as the additive in the electrolyte, which is much higher than that without  $\text{LiNO}_3$  (829.9 mA h/g). In addition, the capacity of Li-S cell with  $\text{LiNO}_3$  is maintained at 531.5 mA h/g after 19 cycles, equaling to 51.8% of the initial capacity; while the capacity of Li-S cell free of  $\text{LiNO}_3$  is retained at only 162.8 mA h/g (19.6% of its initial capacity). These results clearly demonstrate that  $\text{LiNO}_3$  is an effective additive to improve the cycling performance of Li-S cells.

Fig. 1b and c show the representative discharge/charge voltage profiles of Li-S cells using the electrolyte with and without  $\text{LiNO}_3$  in the voltage window of 1.8–2.6 V at 0.05 C (1 C = 1675 mA/g), respectively. The cell using the electrolyte with  $\text{LiNO}_3$  exhibits two typical discharge plateaus at 2.3 V and 2.1 V, indicating the formation of long chain polysulfides and short chain polysulfides during the discharge process [1,2,36]. The charge voltage profiles also show the plateau at 2.3 V, followed by a steep rise of voltage to the cutoff voltage (2.8 V) [1,2,36]. In contrast, when using the electrolyte without  $\text{LiNO}_3$ , the voltage

profiles show only indistinguishable plateaus, which is probably due to the distorted discharge/charge processes [37]. Overall, these results clearly indicate that the use of  $\text{LiNO}_3$  as additive makes the electrochemical reaction of sulfur reversible during the discharge/charge processes and results in a higher specific capacity, which is consistent with previous reports [11,14,16–18,21,23]. According to the conventional understanding,  $\text{LiNO}_3$  can oxidize the polysulfides and be reduced itself to form a protective  $\text{Li}_x\text{SO}_y/\text{Li}_x\text{NO}_y$  SEI layer between the electrolyte and the lithium anode to suppress the polysulfide shuttle effect and the decomposition of electrolyte [14,21,24].

To better understand the influence of  $\text{LiNO}_3$  on the formation of the SEI layer on lithium anodes, scanning electron microscope (SEM) was employed to obtain the morphology of lithium anodes cycled with and without  $\text{LiNO}_3$  additive. Fig. 2 shows the SEM images of lithium anodes using the electrolyte with the addition of  $\text{LiNO}_3$  after 1st discharge (Figs. 2a and 2b) and 1st charge (Figs. 2c and 2d) and the electrolyte without  $\text{LiNO}_3$  after 1st discharge (Figs. 2e and 2f) and 1st charge (Figs. 2g and 2h), respectively.

After the 1st discharge, the lithium anode cycled with  $\text{LiNO}_3$  shows a relatively smoother and more compact surface compared with that cycled without  $\text{LiNO}_3$  (Figs. 2a and 2b vs. Figs. 2e and 2f), indicating that the reaction between intermediate polysulfides and lithium anodes is alleviated by adding  $\text{LiNO}_3$  in electrolyte [13,21]. The holes observed on the surface of lithium anodes could be induced by the nonuniform extraction of lithium during the discharge process. While after the 1st charge, the surface of the lithium anode cycled with  $\text{LiNO}_3$  still exhibits a relatively smooth morphology with a few protuberances (Figs. 2c and 2d), indicative of the formation of a dense and stable SEI layer due to the complex reaction between lithium metal,  $\text{LiNO}_3$ , and polysulfides [15,21,24]. In contrast, uneven growth of mossy lithium accompanied with apparent cracks in the SEI layer can be clearly observed when using the electrolyte without  $\text{LiNO}_3$  (Figs. 2g and 2h). As a consequence, fresh lithium metal is continuously exposed to the electrolyte during cycling, resulting in the electrolyte decomposition and rapid loss of lithium metal and electrolyte [13]. This finding is consistent with previous reports showing that the reaction products ( $\text{Li}_2\text{S}$ ) of polysulfides and lithium metal can induce heterogeneities of the lithium metal surface and thus aggravate electrolyte decomposition and lithium dendrite formation [13,38]. Overall, the SEM results provide a direct evidence that  $\text{LiNO}_3$  strongly affects the morphology and thus the surface chemistry of the SEI layer on lithium anodes, which can greatly influence the cycling performance of Li-S cells.

In order to further understand the influence of  $\text{LiNO}_3$  on the surface chemistry of SEI layer formed on lithium anodes, *operando* S K-edge XAS experiments were performed throughout the first discharge process of Li-S cells using the electrolyte with and without  $\text{LiNO}_3$  additive. Figs. 3a and 3b show the *operando* S K-edge XAS spectra of Li-S cells using electrolyte with and without  $\text{LiNO}_3$  throughout the first discharge process, respectively. For convenience of

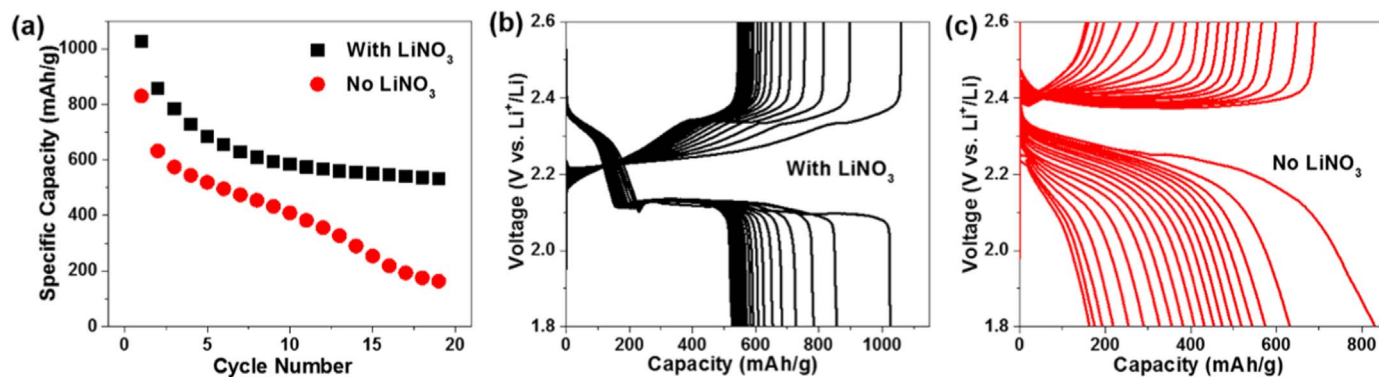
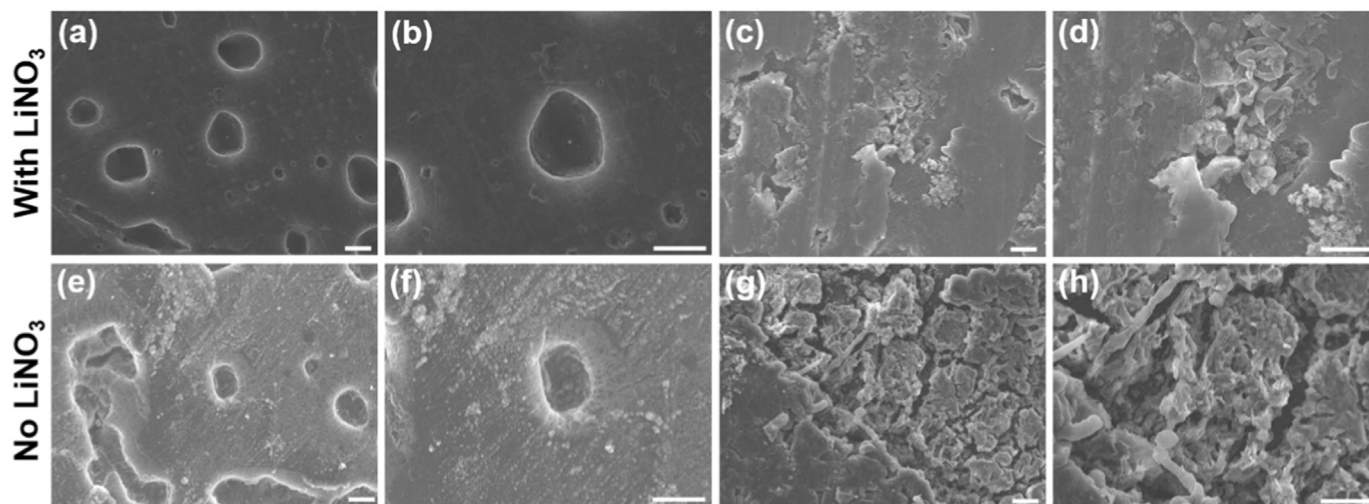


Fig. 1. (a) Cycling performance of Li-S cells with  $\text{LiNO}_3$ -containing and  $\text{LiNO}_3$ -free electrolyte. (b, c) Voltage profiles of Li-S cells with  $\text{LiNO}_3$ -containing and  $\text{LiNO}_3$ -free electrolyte for the first 19 cycles.



**Fig. 2.** SEM images of lithium anodes in Li-S cells cycled with  $\text{LiNO}_3$ -containing electrolyte after 1st discharge (a, b) and 1st charge (c, d), and with  $\text{LiNO}_3$ -free electrolyte after 1st discharge (e, f) and 1st charge (g, h). The scale bar is 20  $\mu\text{m}$ .

comparison, the S K-edge XAS spectra of the initial and final discharge stages and the reference spectrum of LiTFSI are shown in Fig. 3c.

The feature at 2472.2 eV originates from the elemental sulfur or neutral sulfur in polysulfides [30,34], which is observed at the very beginning of the discharge process (the bottom spectra in Figs. 3a and 3b) for both investigated systems. In principle, this feature should not be detected initially as the incoming X-ray directly penetrates through the electrolyte considering the specific design of our *operando* cell (Figure S1 in Supporting information). The observation of this feature therefore indicates the dissolution of limited sulfur into electrolyte due to the imperfect confinement of active materials by PVDF binder [39,40]. In addition, a new feature at 2470.5 eV identified as the fingerprint of charged sulfur in polysulfides [30,34,41] appears at the intermediate stages of discharge, which can be attributed to the

dissolved polysulfides in electrolyte. These polysulfides give rise to the shuttle effect, resulting in poor cycling performance and active material loss. However, the intensity of this feature is much weaker when using electrolyte without  $\text{LiNO}_3$ , which will be discussed later. The feature at 2480.0 eV is attributed to the sulfonyl groups in LiTFSI [42]. The distinct difference between the XAS spectra of these two cells can be found for the features near 2480.0 eV: when adding  $\text{LiNO}_3$  in the electrolyte, two new peaks appear at 2478.0 and 2482.0 eV during the discharge process, which are assigned to  $\text{Li}_2\text{SO}_3$  and  $\text{Li}_2\text{SO}_4$  species, respectively [43–45]; whereas no such feature is observed when using  $\text{LiNO}_3$ -free electrolyte. As both  $\text{Li}_2\text{SO}_3$  and  $\text{Li}_2\text{SO}_4$  are insoluble in the electrolyte, they must come from the SEI layer formed on the surface of lithium anodes rather than the electrolyte or the separator [46]. These results also indicate the presence of  $\text{Li}_2\text{SO}_3$  and

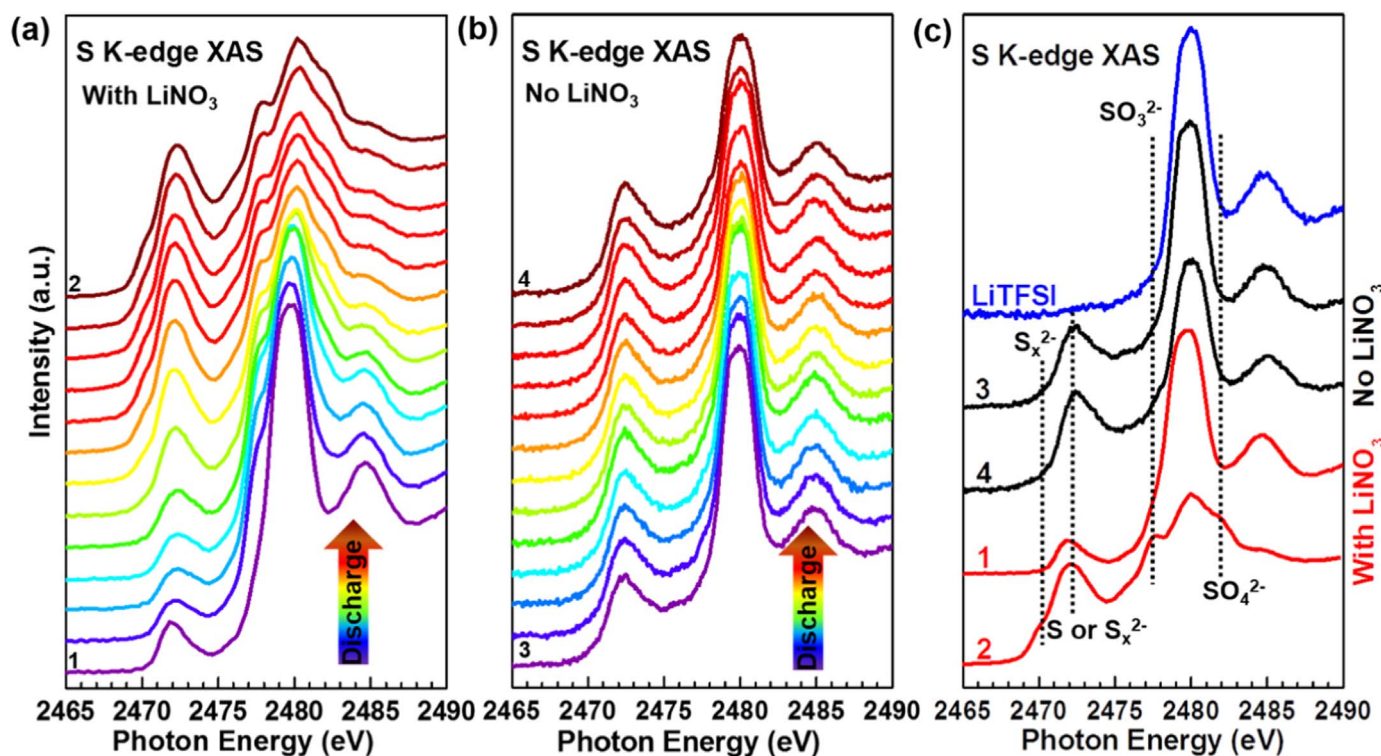


**Fig. 3.** *Operando* S K-edge XAS spectra of Li-S cells using  $\text{LiNO}_3$ -containing (a) and  $\text{LiNO}_3$ -free (b) electrolyte during the 1st discharge process. (c) Comparison of S K-edge XAS spectra of the initial and final discharge stages of 1st discharge process. The spectrum of LiTFSI is also shown as a reference.

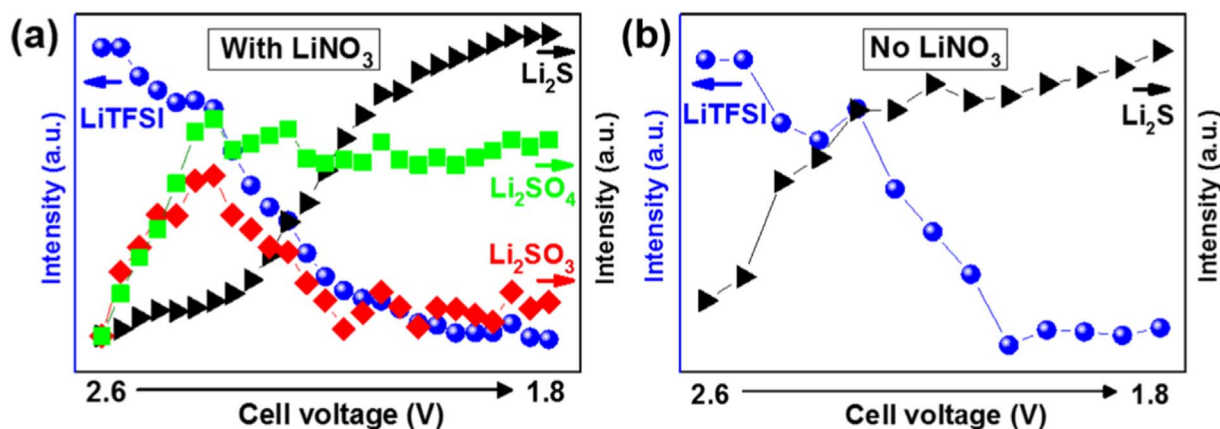


Fig. 4. Evolution of different sulfur species for Li-S cells with  $\text{LiNO}_3$ -containing (a) and  $\text{LiNO}_3$ -free (b) electrolyte during the 1st discharge process.

$\text{Li}_2\text{SO}_4$  in the SEI layer is related with the  $\text{LiNO}_3$  additive.

To demonstrate more clearly how the SEI layer is developed throughout the 1<sup>st</sup> discharge process, we have plotted the normalized intensity of different sulfur species, *i.e.*,  $\text{LiTFSI}$ ,  $\text{Li}_2\text{SO}_3$ ,  $\text{Li}_2\text{SO}_4$ , and  $\text{Li}_2\text{S}$ , for Li-S cells using electrolyte with and without  $\text{LiNO}_3$ , as shown in Fig. 4. Note that the content of  $\text{Li}_2\text{S}$  is represented by the normalized intensity related to  $\text{Li}_2\text{S}$  feature at 2475.7 eV [40]. For both samples, the content of  $\text{LiTFSI}$  decreases gradually during the discharge process as a result of the increased polysulfide concentration in the electrolyte. Moreover, the possible decomposition of  $\text{LiTFSI}$  may also contribute to the intensity decrease [11,21]. In contrast, the content of  $\text{Li}_2\text{S}$  increases monotonously as a function of voltage, indicating that the shuttled polysulfides continuously react with lithium metal to form insoluble  $\text{Li}_2\text{S}$  on the surface of lithium anode [13,21,41]. Interestingly, when  $\text{LiNO}_3$  is added to the electrolyte, the intensity of  $\text{Li}_2\text{SO}_4$  increases steadily during the initial discharge stages and then becomes nearly constant. In contrast, the intensity of  $\text{Li}_2\text{SO}_3$  increase initially and then decrease obviously as a function of the discharge voltage.

We further carried out *ex-situ* XAS experiments to understand the origin of  $\text{Li}_2\text{SO}_3$  and  $\text{Li}_2\text{SO}_4$  in the SEI layer. Fig. 5 and Figure S2 in Supporting information show a comparison of the F, N, O, and C K-edge XAS spectra of the SEIs formed on lithium anodes with and without  $\text{LiNO}_3$  additive. The major difference can be found in the N K-

edge XAS spectra (Fig. 5a). A strong N-O peak located at 404.2 eV is observed for the SEIs formed in the electrolyte with  $\text{LiNO}_3$  after 1st discharge and charge processes, whereas this feature does not show up for the SEIs formed without  $\text{LiNO}_3$ . This peak is assigned to N–O bond from the insoluble  $\text{LiNO}_2$  according to its position, indicating the partial reduction of  $\text{LiNO}_3$  [13,21]. The other N-C peak may originate from the reaction product between decomposed electrolyte and  $\text{LiNO}_3$ . In addition, the absence of N signal from the N K-edge spectra of SEIs formed without  $\text{LiNO}_3$  additive indicates the successful removal of electrolyte from the investigated samples, otherwise N signal from  $\text{LiTFSI}$  should be observed. For the F K-edge spectra (Fig. 5b), they show similar spectral features for the SEI layers formed in the electrolyte with and without  $\text{LiNO}_3$ , which can be assigned to F in  $\text{LiF}$  and  $\text{LiCF}_3$  due to the decomposition of  $\text{LiTFSI}$  [11,13]. This observation also indicates that  $\text{LiNO}_3$  is not very related with the decomposition of  $\text{LiTFSI}$ . Furthermore, both C and O K-edge XAS spectra (Figure S2 in Supporting information) confirm the presence of different decomposition products of the electrolyte, *e.g.*,  $\text{Li}_2\text{CO}_3$ ,  $\text{LiCF}_3$ , and  $\text{Li}_2\text{O}$  [11,13,21].

Combining the data shown above with previous reports [13,21,24], we propose the following reaction mechanism for the formation of the protective SEI layer on lithium anode using electrolyte with  $\text{LiNO}_3$  additive (Fig. 6):  $\text{LiNO}_3$  can oxidize the shuttled polysulfides to  $\text{Li}_2\text{SO}_3$

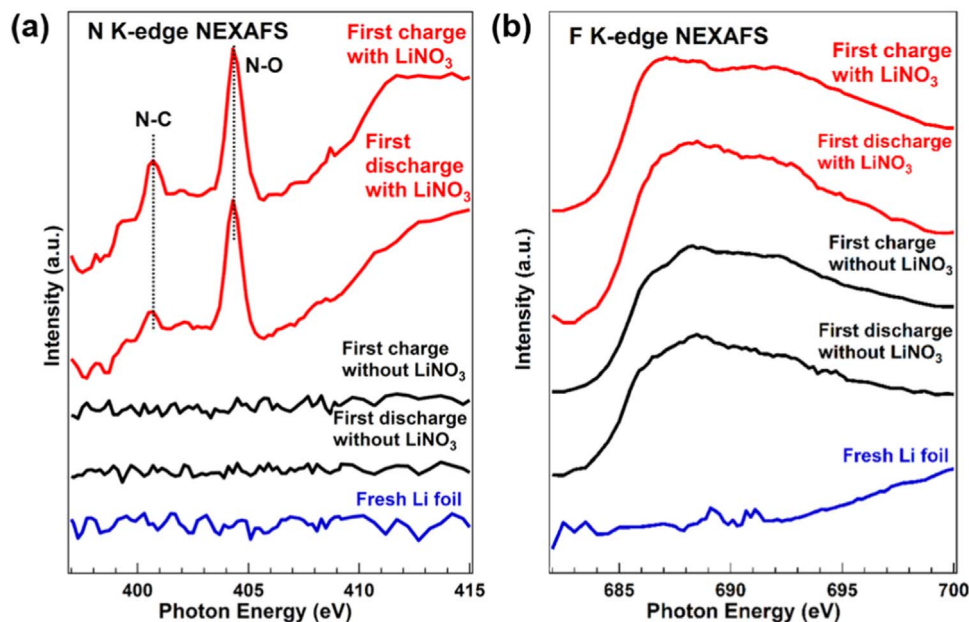


Fig. 5. *Ex-situ* N K-edge (a) and F K-edge (b) XAS spectra of lithium anodes with  $\text{LiNO}_3$ -containing and  $\text{LiNO}_3$ -free electrolyte after 1st discharge and 1st charge processes, respectively.

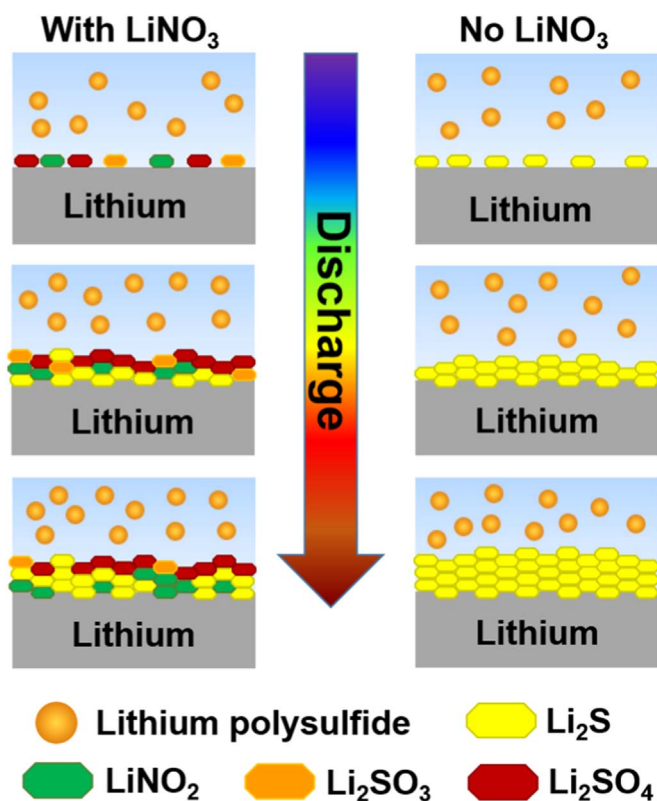
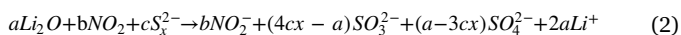


Fig. 6. Schematic illustration of the possible mechanisms of SEI formation on lithium anodes with (left) and without (right)  $\text{LiNO}_3$  additive in electrolyte.

and  $\text{Li}_2\text{SO}_4$  while it is reduced to  $\text{LiNO}_2$  through a two-step reaction (Eqs. (1) and (2)) [24]. At the beginning of the discharge process, these reaction products coprecipitate on lithium anode. With the proceeding of the reactions, the content of  $\text{Li}_2\text{SO}_3$  and  $\text{Li}_2\text{SO}_4$  continues growing until a stable layer composed of these two species is formed on the surface of lithium anode (Fig. 4a and Fig. 6). This surface layer can block the contact between  $\text{LiNO}_3$  in the electrolyte and lithium metal, consequently reaction (1) is prohibited. The gradual decrease of the  $\text{Li}_2\text{SO}_3$  content in the subsequent discharge stages (Fig. 4a) is very likely due to the further reaction between  $\text{Li}_2\text{SO}_3$  and  $\text{LiNO}_3$  to form  $\text{Li}_2\text{SO}_4$ , because the sulfur atoms in  $\text{Li}_2\text{SO}_3$  are not in the highest oxidation states [11].



Actually, the presence of this passivation layer can effectively not only prevent the lithium anode from chemical reaction with polysulfides dissolved in the electrolyte but also suppress the polysulfides from electrochemical reduction on the lithium surface, resulting in the alleviation of polysulfide shuttle effect [13,14,38,47,48]. Note that certain defect states could be formed during the formation process of this surface layer. It is possible that partial polysulfides can still intercalate into the interface of passivation layer/lithium anode through the defect states and react with the lithium metal to form  $\text{Li}_2\text{S}$ . In that case, the content of  $\text{Li}_2\text{S}$  should also increase during the discharge process, which is in good agreement with the *operando* XAS results. Note that due to the presence of defect states in the formed SEI layer, the interaction between polysulfides and lithium anodes can not be totally eliminated, which can result in the irreversible capacity loss. This is consistent with the cycling performance of Li-S battery using the electrolyte with  $\text{LiNO}_3$ : the specific capacity is slowly decaying with increasing the cycle number, although the cycling performance is still superior to that using the electrolyte without  $\text{LiNO}_3$  (Fig. 1). The nearly

constant intensity of  $\text{Li}_2\text{SO}_4$  in the later discharge process also indicates that the formed  $\text{Li}_2\text{S}$  is mainly located underneath the passivation layer (Fig. 4a and Fig. 6). Therefore, the intermediate polysulfides are considered as a double-edged sword in Li-S batteries: on the one hand, it can react with lithium metal to form  $\text{Li}_2\text{S}$  in the anode side, resulting in the irreversible loss of active materials; on the other hand, the polysulfides and  $\text{LiNO}_3$  additive have a synergetic effect on lithium anode, which can form a stable SEI layer on lithium anode and ameliorate the polysulfide shuttle effect and the growth of lithium dendrite. It is worth mentioning that the concentration of polysulfides and the ratio of polysulfides to  $\text{LiNO}_3$  can play an important role on the cycling performance and lithium deposition morphology [22,24]. Therefore, delicate design of sulfur cathode to control the dissolution of intermediate polysulfides into electrolyte (e.g., using functional polymer binders [49–51] and nanostructured metal oxide and sulfides [3,52–54]) is highly required to achieve high-performance Li-S batteries. Ongoing investigations are exploring in situ XAS to unravel the influence of polysulfide concentration and species on the formation process of SEI layer on lithium anode using electrolyte with  $\text{LiNO}_3$ .

In contrast, when using electrolyte without  $\text{LiNO}_3$ , the dissolved polysulfides react with lithium metal to form insulating  $\text{Li}_2\text{S}$  on the surface of lithium anode, leading to the gradual increase of the thickness of the SEI layer (Fig. 6). The thick SEI layer can result in rapid loss of lithium metal and electrolyte as well as lithium dendrite formation, which causes a poor cycling performance of Li-S batteries [13,38]. As a consequence of the continuous consumption of polysulfides in the electrolyte, the polysulfide concentration in the electrolyte is lower compared with that using electrolyte with  $\text{LiNO}_3$ . Therefore, the intensity of polysulfide feature in the XAS spectra should be lower for the former, which is in good agreement with the *operando* XAS results.

### 3. Conclusions

To summarize, we have systematically investigated the influence of  $\text{LiNO}_3$  additive on the formation process of the SEI layer on lithium anode by electrochemical measurements, SEM, *ex-situ* and *operando* XAS. The cycling performance of Li-S cells can be greatly improved by adding  $\text{LiNO}_3$  in the electrolyte. The improved cycling performance is attributed to the synergetic effect of  $\text{LiNO}_3$  and intermediate polysulfides formed during the discharge process:  $\text{LiNO}_3$  can oxidize the shuttled polysulfides to  $\text{Li}_2\text{SO}_3$  and  $\text{Li}_2\text{SO}_4$  while it is reduced to  $\text{LiNO}_2$ , resulting in the formation of a compact and stable layer composed of  $\text{Li}_2\text{SO}_3$  and  $\text{Li}_2\text{SO}_4$  on lithium anode during the initial discharge process. This passivation layer can effectively suppress the reaction between polysulfides and lithium metal, resulting in the alleviation of polysulfide shuttle effect and thus the superior cycling performance. Our present study provides a deeper insight into the role of  $\text{LiNO}_3$  for the suppression of shuttle effect, which can facilitate the development of new electrolyte additives to form defect-free SEI layer on lithium anodes to further improve the cycling performance of Li-S batteries and other lithium metal-anode batteries.

### Acknowledgement

This work was supported by the Assistant Secretary for Energy Efficiency and Renewal Energy under the Battery Materials Research (BMR) program. The work at Advanced Light Source and Molecular Foundry of Lawrence Berkeley National Laboratory was supported by the Director, Office of Science, Office of Basic Energy Sciences, of the U.S. Department of Energy under Contract no. DE-AC02-05CH11231. L.M. acknowledges financial support from National Key Research and Development Program of China (2016YFA0202603), National Natural Science Fund for Distinguished Young Scholars (51425204).

## Appendix A. Supporting information

Supplementary data associated with this article can be found in the online version at doi:10.1016/j.ensm.2017.09.001.

## References

- [1] A. Manthiram, Y. Fu, S.H. Chung, C. Zu, Y.S. Su, *Chem. Rev.* 114 (2014) 11751–11787.
- [2] Y. Yang, G. Zheng, Y. Cui, *Chem. Soc. Rev.* 42 (2013) 3018–3032.
- [3] X. Liu, J.Q. Huang, Q. Zhang, L. Mai, *Adv. Mater.* 29 (2017) 1601759.
- [4] R. Fang, S. Zhao, Z. Sun, D.W. Wang, H.M. Cheng, F. Li, *Adv. Mater.* (2017). <http://dx.doi.org/10.1002/adma.201606823>.
- [5] J.-Q. Huang, Q. Zhang, F. Wei, *Energy Storage Mater.* 1 (2015) 127–145.
- [6] B. Papandrea, X. Xu, Y. Xu, C.-Y. Chen, Z. Lin, G. Wang, Y. Luo, M. Liu, Y. Huang, L. Mai, X. Duan, *Nano Res.* 9 (2016) 240–248.
- [7] Z. Lin, C. Liang, *J. Mater. Chem. A* 3 (2015) 936–958.
- [8] G. Zhou, S. Pei, L. Li, D.W. Wang, S. Wang, K. Huang, L.C. Yin, F. Li, H.M. Cheng, *Adv. Mater.* 26 (625–631) (2014) 664.
- [9] G. Zhou, J. Sun, Y. Jin, W. Chen, C. Zu, R. Zhang, Y. Qiu, J. Zhao, D. Zhuo, Y. Liu, X. Tao, W. Liu, K. Yan, H.R. Lee, Y. Cui, *Adv. Mater.* 29 (2017) 1603366.
- [10] Y.V. Mikhaylik, *U.S. Pat. 7646171 B2*, 2010.
- [11] D. Aurbach, E. Pollak, R. Elazari, G. Salitra, C.S. Kelley, J. Affinito, *J. Electrochem. Soc.* 156 (2009) A694.
- [12] X.B. Cheng, R. Zhang, C.Z. Zhao, F. Wei, J.G. Zhang, Q. Zhang, *Adv. Sci.* 3 (2016) 1500213.
- [13] W. Li, H. Yao, K. Yan, G. Zheng, Z. Liang, Y.M. Chiang, Y. Cui, *Nat. Commun.* 6 (2015) 7436.
- [14] S.S. Zhang, J.A. Read, *J. Power Source* 200 (2012) 77–82.
- [15] X. Liang, Z. Wen, Y. Liu, M. Wu, J. Jin, H. Zhang, X. Wu, *J. Power Sources* 196 (2011) 9839–9843.
- [16] S.S. Zhang, *J. Electrochem. Soc.* 159 (2012) A920–A923.
- [17] S.S. Zhang, *J. Power Sources* 322 (2016) 99–105.
- [18] S.S. Zhang, *Electrochim. Acta* 70 (2012) 344–348.
- [19] S. Xiong, K. Xie, Y. Diao, X. Hong, *Electrochim. Acta* 83 (2012) 78–86.
- [20] S. Xiong, K. Xie, Y. Diao, X. Hong, *J. Power Sources* 236 (2013) 181–187.
- [21] S. Xiong, K. Xie, Y. Diao, X. Hong, *J. Power Sources* 246 (2014) 840–845.
- [22] C. Yan, X.-B. Cheng, C.-Z. Zhao, J.-Q. Huang, S.-T. Yang, Q. Zhang, *J. Power Sources* 327 (2016) 212–220.
- [23] R. Xu, J.C.M. Li, J. Lu, K. Amine, I. Belharouak, *J. Mater. Chem. A* 3 (2015) 4170–4179.
- [24] C.-Z. Zhao, X.-B. Cheng, R. Zhang, H.-J. Peng, J.-Q. Huang, R. Ran, Z.-H. Huang, F. Wei, Q. Zhang, *Energy Storage Mater.* 3 (2016) 77–84.
- [25] J. Lu, T. Wu, K. Amine, *Nat. Energy* 2 (2017) 17011.
- [26] L. Mai, M. Yan, Y. Zhao, *Nature* 546 (2017) 469.
- [27] G. Rong, X. Zhang, W. Zhao, Y. Qiu, M. Liu, F. Ye, Y. Xu, J. Chen, Y. Hou, W. Li, W. Duan, Y. Zhang, *Adv. Mater.* 29 (2017) 1606187.
- [28] A. Jozwiuk, B.B. Berkes, T. Weiß, H. Sommer, J. Janek, T. Brezesinski, *Energy Environ. Sci.* 9 (2016) 2603–2608.
- [29] E. Talaie, P. Bonnicks, X. Sun, Q. Pang, X. Liang, L.F. Nazar, *Chem. Mater.* 29 (2016) 90–105.
- [30] M. Cuisinier, P.-E. Cabelguen, S. Evers, G. He, M. Kolbeck, A. Garsuch, T. Bolin, M. Balasubramanian, L.F. Nazar, *J. Phys. Chem. Lett.* 4 (2013) 3227–3232.
- [31] Y. Gorlin, A. Siebel, M. Piana, T. Huthwelker, H. Jha, G. Monsch, F. Kraus, H.A. Gasteiger, M. Tromp, *J. Electrochem. Soc.* 162 (2015) A1146–A1155.
- [32] M.A. Lowe, J. Gao, H.D. Abruña, *RSC Adv.* 4 (2014) 18347.
- [33] K.H. Wujcik, D.R. Wang, T.A. Pascal, D. Prendergast, N.P. Balsara, *J. Electrochem. Soc.* 164 (2016) A18–A27.
- [34] K.H. Wujcik, T.A. Pascal, C.D. Pemmaraju, D. Devaux, W.C. Stolte, N.P. Balsara, D. Prendergast, *Adv. Energy Mater.* 5 (2015) 1500285.
- [35] L. Zhang, D. Sun, J. Feng, E.J. Cairns, J. Guo, *Nano Lett.* 17 (2017) 5084–5091. <http://dx.doi.org/10.1021/acs.nanolett.7b02381>.
- [36] Z.W. Seh, Y. Sun, Q. Zhang, Y. Cui, *Chem. Soc. Rev.* 45 (2016) 5605–5634.
- [37] Y.V. Mikhaylik, J.R. Akridge, *J. Electrochem. Soc.* 151 (2004) A1969.
- [38] C. Zu, A. Manthiram, *J. Phys. Chem. Lett.* 5 (2014) 2522–2527.
- [39] P.P.R.M.L. Harks, C.B. Robledo, T.W. Verhallen, P.H.L. Notten, F.M. Mulder, *Adv. Energy Mater.* 7 (2017) 1601635.
- [40] Y. Gorlin, M.U.M. Patel, A. Freiberg, Q. He, M. Piana, M. Tromp, H.A. Gasteiger, *J. Electrochem. Soc.* 163 (2016) A930–A939.
- [41] T.A. Pascal, K.H. Wujcik, J. Velasco-Velez, C. Wu, A.A. Teran, M. Kapilashrami, J. Cabana, J. Guo, M. Salmeron, N. Balsara, D. Prendergast, *J. Phys. Chem. Lett.* 5 (2014) 1547–1551.
- [42] M.U. Patel, I. Arcon, G. Aquilanti, L. Stievano, G. Mali, R. Dominko, *ChemPhysChem* 15 (2014) 894–904.
- [43] A. Braun, M. Janousch, J. Sfeir, J. Kiviahio, M. Noponen, F.E. Huggins, M.J. Smith, R. Steinberger-Wilckens, P. Holtappels, T. Graule, *J. Power Sources* 183 (2008) 564–570.
- [44] N. Kornienko, J. Resasco, N. Becknell, C.M. Jiang, Y.S. Liu, K. Nie, X. Sun, J. Guo, S.R. Leone, P. Yang, *J. Am. Chem. Soc.* 137 (2015) 7448–7455.
- [45] X. Feng, M.K. Song, W.C. Stolte, D. Gardenghi, D. Zhang, X. Sun, J. Zhu, E.J. Cairns, J. Guo, *Phys. Chem. Chem. Phys.* 16 (2014) 16931–16940.
- [46] Z. Liu, S. Bertolini, P.B. Balbuena, P.P. Mukherjee, *ACS Appl. Mater. Inter.* 8 (2016) 4700–4708.
- [47] X.-B. Cheng, C. Yan, X. Chen, C. Guan, J.-Q. Huang, H.-J. Peng, R. Zhang, S.-T. Yang, Q. Zhang, *Chem* 2 (2017) 258–270.
- [48] X.-B. Cheng, C. Yan, H.-J. Peng, J.-Q. Huang, S.-T. Yang, Q. Zhang, *Energy Storage Mater.* (2017). <http://dx.doi.org/10.1016/j.ensm.2017.03.008>.
- [49] W. Li, Q. Zhang, G. Zheng, Z.W. Seh, H. Yao, Y. Cui, *Nano Lett.* 13 (2013) 5534–5540.
- [50] W. Chen, T. Qian, J. Xiong, N. Xu, X. Liu, J. Liu, J. Zhou, X. Shen, T. Yang, Y. Chen, C. Yan, *Adv. Mater.* 29 (2017) 1605160.
- [51] C. Milroy, A. Manthiram, *Adv. Mater.* 28 (2016) 9744–9751.
- [52] H.J. Peng, G. Zhang, X. Chen, Z.W. Zhang, W.T. Xu, J.Q. Huang, Q. Zhang, *Angew. Chem. Int. Ed.* 55 (2016) 12990–12995.
- [53] X. Liang, C. Hart, Q. Pang, A. Garsuch, T. Weiss, L.F. Nazar, *Nat. Commun.* 6 (2015) 5682.
- [54] X. Tao, J. Wang, C. Liu, H. Wang, H. Yao, G. Zheng, Z.W. Seh, Q. Cai, W. Li, G. Zhou, C. Zu, Y. Cui, *Nat. Commun.* 7 (2016) 11203.